SIAM J. NUMER. ANAL.
Vol. 31, No. 3, pp. 788–812, June 1994

011

THE ACCURACY OF NUMERICAL CONFORMAL MAPPING METHODS: A SURVEY OF EXAMPLES AND RESULTS*

THOMAS K. DELILLO†

Abstract. This paper shows how the geometry of the region affects the conditioning and the accuracy of numerical conformal mapping methods for simply connected regions, especially Fourier series methods. Both explicit examples of popular test cases and more general estimates are discussed. The severe ill conditioning that is known as the crowding phenomenon is discussed and its effect on a conformally transplanted boundary value problem is illustrated. Remarks on various numerical methods are included.

Key words. numerical conformal mapping, crowding, Fourier series methods

AMS subject classifications. 30C30, 65E05

1. Introduction. The accuracy of numerical approximations of conformal maps is influenced by two properties of the boundary curve: the local property of smoothness and the global property of shape. We will be concerned here mainly with maps between the unit disk and simply connected regions bounded by Jordan curves and mainly with methods that approximate the Taylor series of such maps from the disk. There are a variety of results, some classical, that say that a conformal map can be extended to the boundary with, roughly, the same smoothness as the boundary. These results may be used, for instance, in a standard fashion, to show the rate of decay of the Taylor coefficients of the map. We discuss such a case below. The effect of the global shape of the boundary is less well known and may be much more dramatic. The map from the disk to an elongated region, such as the interior of a slender ellipse, has relative distortions which vary exponentially with the aspect ratio of the region. This severe ill conditioning, known as the crowding phenomenon for the map to the disk (or the Geneva effect in [25, p. 428], presumably because positions that were far apart were drawn close together) was apparently first noticed independently by [17, p. 179], [21, §3], and [31]. It can make the numerical problem difficult or impossible to solve and has been the object of much recent study; see [6], [9]–[12], [19], [20], [28], [30], [33], [35]–[42], [44], [46, p. 4], [52], [53], [55], and [56]. The map from the disk to a "pinched" region, such as the interior of an inverted ellipse, will also suffer from ill conditioning of a less severe, algebraic nature. We will illustrate both these cases in our examples and estimates below.

In this paper we give a detailed discussion and survey of the above effects with a focus on Fourier series methods that approximate the Taylor series of the map from the disk to the region. In this case, the crowding for extreme regions is actually an expansion or spreading of the boundary, but we shall continue to call it "crowding." As shown in [15], [30], and [55], for instance, extreme regions may require an inordinately large number of Fourier coefficients, if they can be mapped at all; see also [22]. If we

* Received by the editors June 17, 1991; accepted for publication (in revised form) April 7, 1993. The author's research was partially supported by U. S. Department of Energy grant DE-FG02-92ER25124 and National Science Foundation grant OSR-9255223 under the National Science Foundation EPSCoR Program.

† Department of Mathematics and Statistics, The Wichita State University, Wichita, Kansas 67260-0033.

think of the problem as one of resolution, then images of the discrete Fourier points do not resolve extreme boundaries well. In this sense maps to the disk are not so badly affected; see [33]. Thus, a Fourier series map from the disk to the interior of an ellipse of major to minor axis ratio 5 is difficult to produce, whereas finding the preimages of the corners of a rectangle for the Schwarz–Christoffel map to the disk becomes difficult for rectangles of aspect ratio 10 or 20; see [47].

In the remainder of this section we will give some introductory results, including a proof of *Zemach's rule* for the smallest number of Taylor coefficients required for even a first order approximation. In §2, we discuss several popular test cases in detail and show that for families of analytic boundary curves whose nearest singularities outside the disk are known, a more precise form of Zemach's rule can be stated. In §3, we discuss some more general attempts to estimate the crowding, including results of Dubiner, Gaier, Pfluger, Wegmann, and Zemach and recent related work on domain decomposition methods for computing conformal modules. In §4, we show how the crowding can affect a numerical solution to a boundary value problem when it is conformally transplanted to the disk. Finally, in §5, we make some remarks on various other numerical methods, including some recent attempts to avoid the crowding problem by picking more appropriate computational domains.

First, let us define some notation: f will denote the conformal map from the interior of the unit disk D to the interior Ω of a Jordan curve Γ with a parametric representation $\gamma = \gamma(\sigma)$, where $0 \le \sigma \le L$ and σ is, for instance, the arclength or polar angle. Also, f will be normalized by $f(0) = a_0$ and either $f'(0) > 0$ or $f(1)$ fixed. Often we will want to consider maps $f = f_\alpha$ to a family of curves $\Gamma_\alpha : \gamma_\alpha(\sigma)$ where $0 < \alpha \le 1$ and α measures the "thinness" of the region or the distance from $f(0)$ to the boundary. For example, Γ_α might be the family of ellipses of minor-to-major axis ratio α centered at the origin with $a_0 = 0$ and major axis [-1,1]. Note that if $\gamma(\sigma)$ is smooth, then f extends smoothly to the boundary of the unit disk and $f(e^{it}) = \gamma(\sigma(t))$, where $\sigma(t)$ is the *boundary correspondence function.* An easy, standard calculation with the Cauchy integral formula shows that the Fourier coefficients of $f(e^{it})$ are the Taylor coefficients, a_k, of f expanded about 0. That is, for $|z| \le 1$, $f(z) = \sum_{k=0}^{\infty} a_k z^k$. We will imagine approximating f by its truncated Taylor series, $f_N(z) = \sum_{k=0}^{N} a_k z^k$. Numerical methods, such as those due to Theodorsen, Fornberg, and Wegmann, essentially produce approximate values $\tilde{a}_k$ to the $N+1$ a_k's. The map obtained by using these approximate coefficients in the truncated series will be denoted by $\tilde{f}_N(z)$. We will consider mainly the effects of the boundary on the accuracy of f_N, since the effects on $\tilde{f}_N$ are similar.

Most numerical conformal mapping methods are essentially methods for solving integral equations for $\sigma(t)$ (or $t(\sigma)$ for maps to the disk). For instance, for Theodorsen's method, we start with the *auxiliary function,* $h(z) = \log f(z)/z$, analytic in D. If Γ is star-shaped with respect to 0, then $\gamma(\sigma) = \rho(\sigma)e^{i\sigma}$ and $h(e^{it}) = \log \rho(\sigma(t)) + i(\sigma(t) - t)$. Let $\mathbf{K}$ denote the conjugation operator relating conjugate harmonic functions Re h and Im h on the boundary of the unit disk, Im $h(e^{it})$ − Im $h(0)$ = $\mathbf{K}$ Re $h(e^{it})$. Using the normalization $f'(0) > 0$ and the representation of $\mathbf{K}$ as a singular integral operator, we have the *Theodorsen integral equation,*

$$\sigma(t) - t = \mathbf{K}(\log \rho(\sigma(t))) = \frac{1}{2\pi} PV \int_0^{2\pi} \cot\left(\frac{t - \tilde{t}}{2}\right) \log \rho(\sigma(\tilde{t}))\, d\tilde{t}.$$

Note that although $\mathbf{K}$ is a linear operator, the equation is nonlinear in $\sigma(t)$ (or,

more properly, in the 2π-periodic function $\sigma(t) - t$) with the nonlinearity entering through the "curve information," $\log \rho(\sigma)$. A method of successive conjugation can be applied to solve the equation. The discretization $\mathbf{K}_N$ of $\mathbf{K}$ can be accomplished by N-point trigonometric interpolation, and the numerical evaluation of $\mathbf{K}_N h(e^{it})$ can be implemented with two N-point FFTs. For a thorough discussion of the basis of the various Fourier series methods in function conjugation, see [23]. For similar discussions and other methods, see, for instance, [5], [16], and [25]. For collections of recent papers and applications, see [37], [45], and [46].

If Γ is analytic, then the Taylor series for f about 0 can be extended outside the unit disk to a radius $R > 1$ equal to the modulus of the nearest singularity to $|z| = 1$. f may also fail to be conformal if $f'(z) = 0$ for some $1 < |z| \leq R$. For a proof of these statements, see [44, p. 41]. We will discuss the case of analytic Γ more thoroughly in the context of our examples in §2.

In practical cases Γ may be considerably less smooth than the analytic cases discussed in our examples. For instance, Γ may be determined by interpolating a set of points by a periodic cubic spline. Theorem 2 gives a result showing how the error in approximating f by f_N depends on N for spline boundaries. In our error estimates we will mainly use the max-norm $\|f\|_\infty = \max_{|z|\leq 1}|f(z)|$. Other results yielding slightly sharper estimates or using different smoothness assumptions or norms are also possible. We will not pursue such details further here. We will, however, need a theorem that guarantees that the extension of f to the boundary of the disk is roughly as smooth as the boundary parametrization, $\gamma(\sigma)$. There are many such results in the literature; see, for instance, [44, Chap. 3] and [23, §4]. Theorem 1 states a result from [23, §4] which applies to the case where Γ is a cubic spline. Let us first define the Sobolev space,

$$W^{m,p} := \{h \text{ periodic; } h^{(m-1)} \text{ absolutely continuous, } h^{(m)} \in L^p\},$$

$$m \geq 1,\ 1 \leq p \leq \infty.$$

THEOREM 1. $\gamma(\sigma) \in W^{m,\infty} \Rightarrow f(e^{it}) \in W^{m,p}, 1 < p < \infty$.

If γ is a cubic spline, then $\gamma^{(2)}$ is absolutely continuous and $\gamma^{(3)}$ is piecewise constant and, hence, in L^∞. Thus $\gamma \in W^{3,\infty}$, and the theorem says $f \in W^{3,p}$ for $1 < p < \infty$. A standard integration-by-parts argument gives the decay of the Fourier coefficients, $|a_k| \leq \|f^{(3)}\|_p/k^3$.

THEOREM 2. *If γ is a cubic spline, then $\|f - f_N\|_\infty \leq CN^{-5/2}$.*

Proof. Using $p = 2$ and the isometry of l_2 and L^2 we have

$$\begin{aligned}\|f - f_N\|_2^2 &= \sum_{k=N+1}^{\infty} |a_k|^2 \\ &= \sum_{k=N+1}^{\infty} |k(k-1)(k-2)a_k|^2 (k(k-1)(k-2))^{-2} \\ &\leq \|f^{(3)}\|_2^2 ((N+1)N(N-1))^{-2}.\end{aligned}$$

Similarly

$$\|f' - f_N'\|_2^2 \leq \|f^{(3)}\|_2^2/((N+1)N)^2.$$

By Warschawski's inequality [16, p. 68],

$$\|f - f_N\|_\infty^2 \leq \frac{1}{2\pi}\|f - f_N\|_2^2 + \frac{1}{2}\|f' - f_N'\|_2 \|f - f_N\|_2 \leq CN^{-5}. \qquad \square$$

Next we state a rule of thumb due to Zemach [55], [56] giving a lower bound on the number of Taylor coefficients N required for even a rough approximation to f. Suppose Γ is smooth and L is its arclength. Let $\Delta t = 2\pi/N$. If N is large enough so that $\frac{\Delta\sigma}{\Delta t} \approx \frac{d\sigma}{dt}$ for all t, then $|f'(e^{it})| = \frac{d\sigma}{dt} \approx \frac{\Delta\sigma}{\Delta t} \leq \frac{NL}{2\pi}$ for all t. That is, for N large enough that f'_N is a good approximation to f', we must have *Zemach's rule*:

$$N \geq \frac{2\pi \|f'\|_\infty}{L}.$$

Note that this expression scales with L. As will be shown below, $\|f'\|_\infty$ may be large for thin regions, so this rule links accuracy to global shape. We will give a more precise statement of this rule for the examples in the next section.

2. Examples. In this section we give the details of some popular test cases and illustrative examples. These examples involve parametrized families of analytic boundaries. We exhibit the Taylor series for the maps and relate the modulus R of the nearest singularity to $\|f'\|_\infty$. This allows us to give our more precise version of Zemach's rule.

For each example, computations with Wegmann's method are reported. As in [50], we find

$$\|f - \tilde{f}_N\|_\infty \approx CR^{-N/2},$$

where the error is measured at the mesh points, $t_j = 2\pi j/N$. The dashed lines in Figs. 2, 4, 6, 8, and 10 indicate the values of $CR^{-N/2}$. The symbols nearby indicate the errors, $\|f - \tilde{f}_N\|_\infty$. The values of C are given below. The error in truncating the exact series after N terms would be $\|f - f_N\|_\infty = O(R^{-N})$, and we might expect the numerical error to be of this order. However, as shown in [18] and as illustrated in the explicit example given in (ii) below, $\|(\mathbf{K} - \mathbf{K}_N)f\|_\infty = O(R^{-N/2})$. This is, indeed, what is found numerically. Roughly speaking, the numerical methods using N mesh points compute $N/2 + 1$ Taylor coefficients accurately. A more careful discussion of the error in $\tilde{f}_N$ would require use of the Sobolev norm as in [50]. In Figs. 1, 3, 5, 7, and 9, images of radial lines and concentric circles in the unit disk are plotted. For the concentric circles with an N-point map, the images of $4N$ equally-spaced points are plotted. If N is not large enough for high accuracy, oscillations may be seen on the boundary, as in Fig. 3 for $\alpha = .2$ (where the accuracy had degraded, as discussed in (ii)) and Fig. 9 for $\alpha = .3$. As noted at the end of this section, the interior of the map may look quite good even for very poor solutions.

(i) *Circle*; see Fig. 1. Γ is the unit circle. Let $0 < \alpha \leq 1$. Then f will just be the Moebius transformation of the unit disk to itself that takes 0 to $-1 + \alpha$. We note the following facts:

$$f(z) = \frac{z - 1 + \alpha}{1 - (1 - \alpha)z} = -1 + \alpha + \alpha(2 - \alpha)\sum_{k=1}^{\infty}(1 - \alpha)^{k-1}z^k,$$

$$R = \frac{1}{1 - \alpha} = 1 + \alpha + O(\alpha^2),$$

$$f' \neq 0,$$

$$\|f'\|_\infty = |f'(1)| = \frac{2}{\alpha} - 1,$$

$$\min_{|z|\leq 1} |f'(z)| = |f'(-1)| = \frac{\alpha}{2 - \alpha}.$$

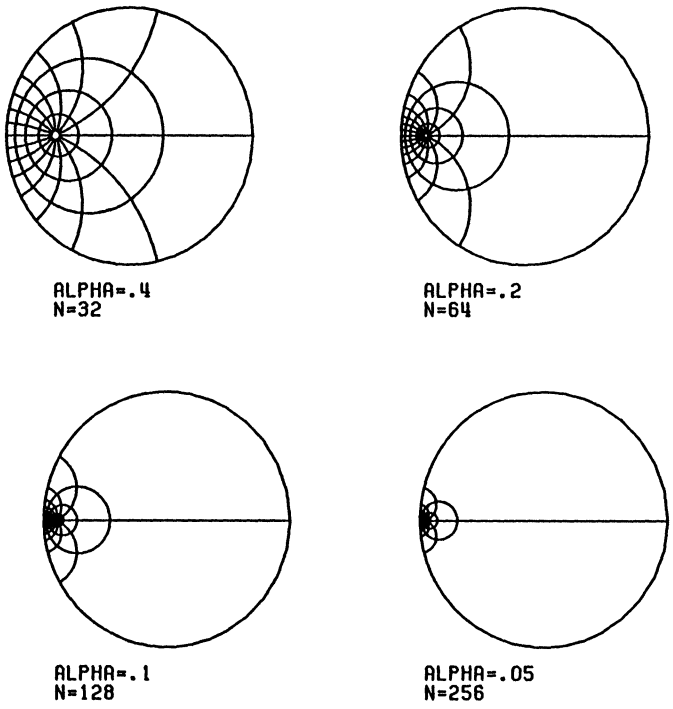

FIG. 1. *Circles with Wegmann's method.*

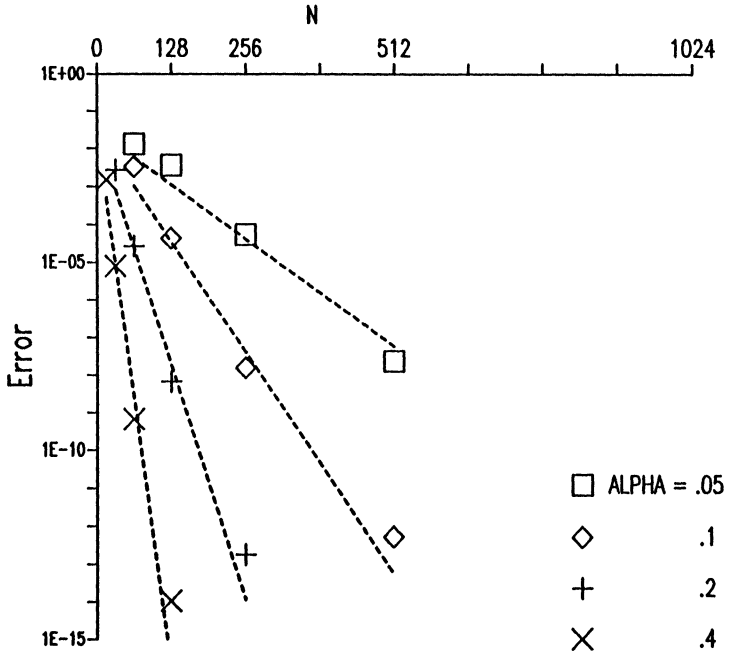

FIG. 2. *Discretization errors for Wegmann's method for circles.*

The errors in Fig. 2 fit the estimate quite well with $C = .03$ for a wide range of α. The degradation of the errors for $\alpha = .2, N = 256$ and $\alpha = .1, N = 512$ is associated with the onset of divergence as discussed at the end of the next example.

(ii) *Inverted ellipse*; see Fig. 3. Here $\Gamma : \gamma(\sigma) = \rho(\sigma)e^{i\sigma}$, where $\rho(\sigma) = \sqrt{1-(1-\alpha^2)\sin^2\sigma}$ for $0 \le \sigma \le 2\pi$ and $0 < \alpha \le 1$. This map is derived by inverting the familiar Joukowski map to the exterior of an ellipse. We note the following

$$f(z) = \frac{2\alpha z}{1+\alpha-(1-\alpha)z^2} = \frac{2\alpha}{1+\alpha}\sum_{k=0}^{\infty}\left(\frac{1-\alpha}{1+\alpha}\right)^k z^{2k+1},$$

$$R = \sqrt{\frac{1+\alpha}{1-\alpha}} = 1+\alpha+O(\alpha^2),$$

$$f'(\pm iR) = 0,$$

$$\|f'\|_\infty = |f'(\pm 1)| = \frac{1}{\alpha},$$

$$\min_{|z|\le 1}|f'(z)| = |f'(\pm i)| = \alpha^2.$$

The exact boundary correspondence is

$$\sigma(t) = \arctan\,\alpha\,\tan(t-\pi/2) - \pi/2.$$

Following the example for the exterior problem for the ellipse in [8] and using the auxiliary function for Theodorsen's method, $h(z) = \log(f(z)/z)$, and $\operatorname{Im} h(e^{it}) = \mathbf{K}\operatorname{Re} h(e^{it})$ with f as given, we have

$$\log\rho(\sigma(t)) = \log\frac{2\alpha}{1+\alpha} + R^{-2}\cos 2t + \frac{R^{-4}}{2}\cos 4t + \cdots,$$

$$\sigma(t) - t = R^{-2}\sin 2t + \frac{R^{-4}}{2}\sin 4t + \cdots.$$

Noting that $\sin mt = \mathbf{K}(\cos mt)$ and that the N-point FFT gives the approximation

$$\log\rho(\sigma(t)) \approx \log\frac{2\alpha}{1+\alpha} + R^{-2}\cos 2t + \frac{R^{-4}}{2}\cos 4t + \cdots + \frac{R^{-N/2}}{N/4}\cos\frac{N}{2}t$$

to the first $N/2$ terms of the sin/cos series, we see that $\|(K-K_N)\log\rho(\sigma(t))\|_\infty \approx O(R^{-N/2})$. This is an explicit example of the estimate in [18]. As is shown in Fig. 4, the errors for Wegmann's method exhibit the same behavior with $C = 1$, at least for $\alpha \ge .4$. For smaller α the errors degrade. This is due to the onset of divergence caused by amplification of rapidly oscillating terms. This "convergence/divergence" phenomenon was noted in [8]. It is discussed in [49] and [50] where cutting off the higher indexed Fourier coefficients in the calculation of the Newton updates is recommended. We have not done this here. Rather, for $\alpha = .2$ we have used an $O(1/N)$ perturbation of the exact boundary correspondence as our initial guess. The first few iterations converge rapidly and then the iterations diverge. We note that the data from Table 1 of [49, p. 323] for the inverted ellipse with $\alpha = .2$ (p=.8 in [49]) with damping of rapid oscillations would be nearer to our predicted values.[1]

[1] Note added in proof: The method given in R. Wegmann [*Discrete Riemann–Hilbert problems, interpolation of simply closed curves, and numerical conformal mapping*, J. Comput. Appl. Math., 23 (1988), pp. 323–352] overcomes these problems.

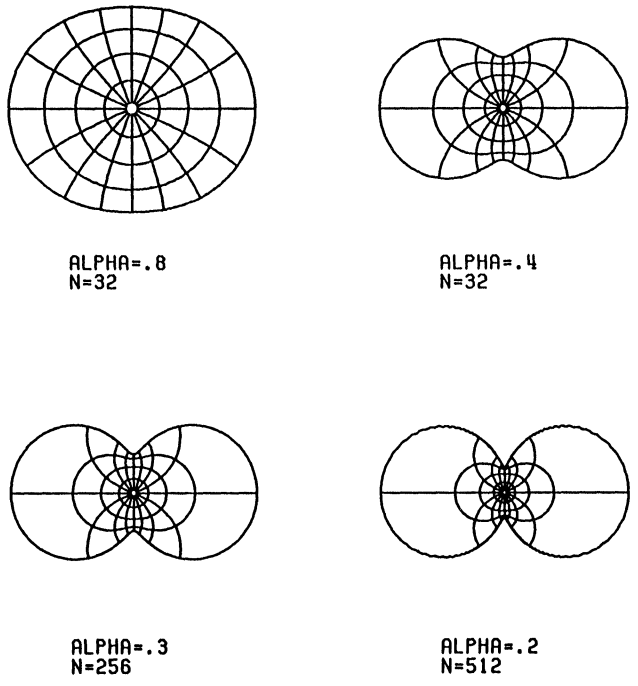

FIG. 3. *Inverted ellipses with Wegmann's method.*

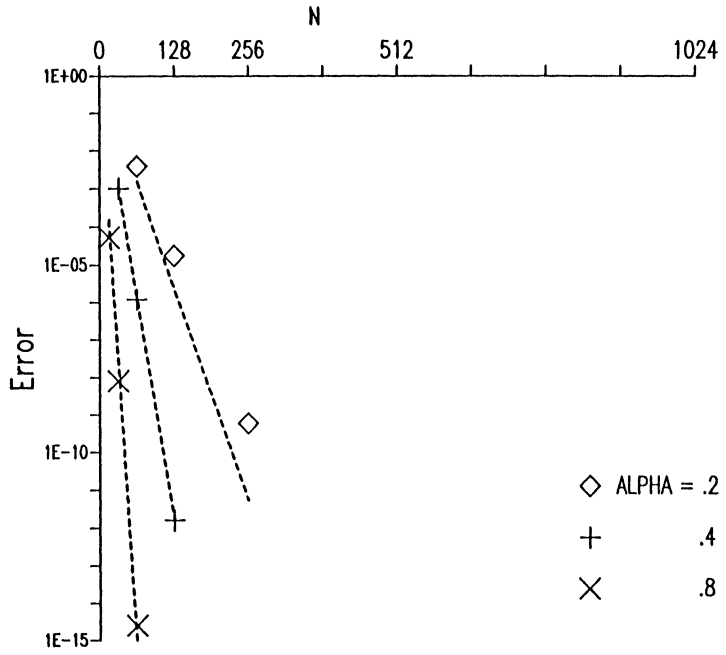

FIG. 4. *Discretization errors for Wegmann's method for inverted ellipses.*

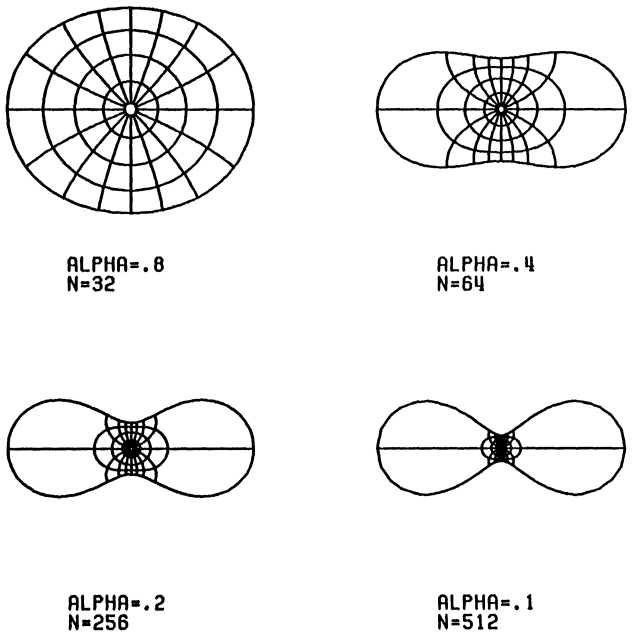

FIG. 5. *Cassini ovals with Wegmann's method.*

(iii) *Cassini oval*; see Fig. 5. Here $\Gamma : \gamma(\sigma) = \rho(\sigma)e^{i\sigma}$ where

$$\rho(\sigma) = \frac{1}{\sqrt{2}}\sqrt{(1-\alpha^2)\cos 2\sigma + \sqrt{(1-\alpha^2)^2\cos^2 2\sigma + 4\alpha^2}}$$

$$\text{for } 0 \le \sigma \le 2\pi \quad \text{and} \quad 0 < \alpha \le 1.$$

We note that

$$f(z) = \alpha z\left(\frac{2}{1+\alpha^2-(1-\alpha^2)z^2}\right)^{\frac{1}{2}} = \left(\frac{2\alpha}{1+\alpha^2}\right)^{\frac{1}{2}}\sum_{k=0}^{\infty}\frac{(2k)!}{(k!)^2 2^{2k}}\left(\frac{1-\alpha^2}{1+\alpha^2}\right)^k z^{2k},$$

$$R = \sqrt{\frac{1+\alpha^2}{1-\alpha^2}} = 1+\alpha^2+O(\alpha^4),$$

$$f' \neq 0,$$

$$\|f'\|_\infty = |f'(\pm 1)| = \frac{1}{2\alpha^2}+\frac{1}{2},$$

$$\min_{|z|\le 1}|f'(z)| = |f'(\pm i)| = \frac{\alpha(1+\alpha^2)}{2}.$$

$C = .01$ gives a reasonably good fit to the data in Fig. 6. Our results with Wegmann's method can be compared to Fornberg's results with his method for the same example given in [15, Table 2]. In terms of our α, his α is $\sqrt{(1-\alpha^2)/(1+\alpha^2)}$. Such a comparison indicates that Wegmann's method is slightly better for (our) α near 1, and Fornberg's method is slightly better for α near 0.

(iv) *Arctanh*; see Fig. 7. Here we investigate an explicit map exploited by Dubiner in his theoretical estimates in [12]. We use the map from the disk to the infinite strip

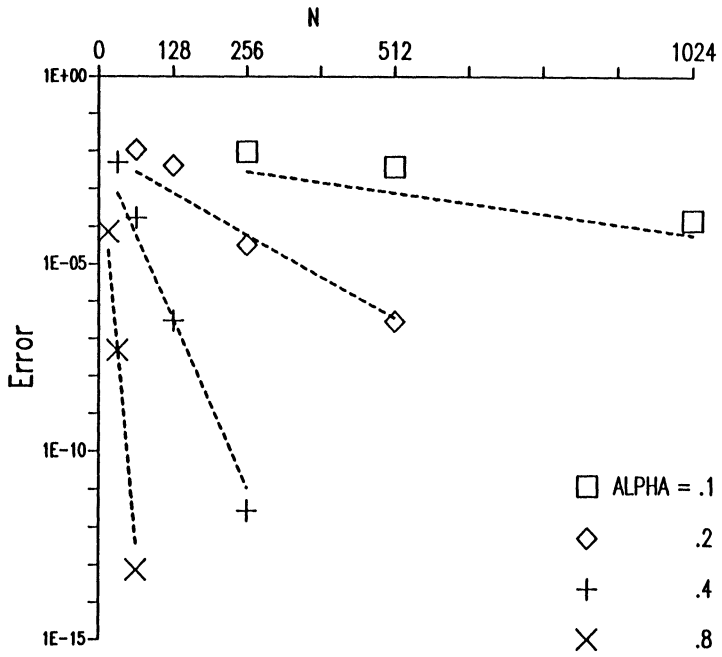

FIG. 6. *Discretization errors for Wegmann's method for Cassini ovals.*

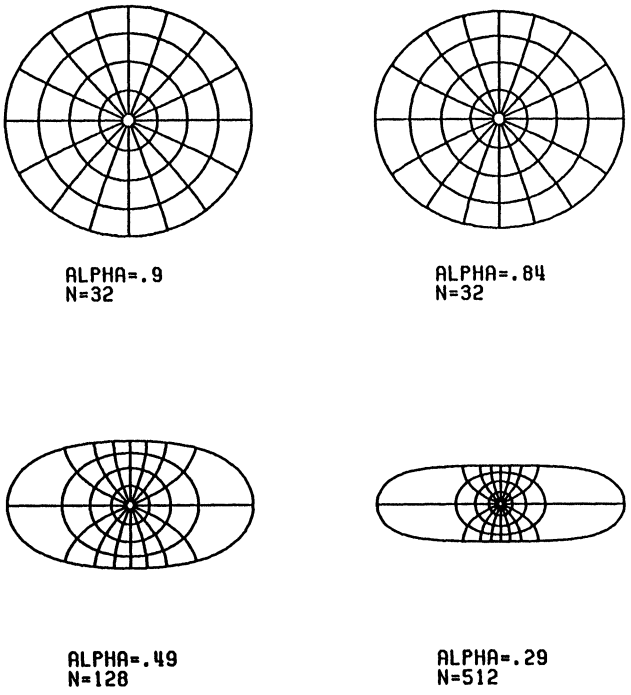

FIG. 7. Arctanh *regions with Wegmann's method.*

normalized as follows:

$$f(z) = \operatorname{arctanh}(1-\beta)z = \frac{1}{2}\log\frac{1+(1-\beta)z}{1-(1-\beta)z} = \sum_{k=1}^{\infty}\frac{1}{2k-1}\left(\frac{z}{R}\right)^{2k-1},$$

$$R = \frac{1}{1-\beta} \quad \text{with } 0<\beta<1,$$

$$f'(z) = \frac{1-\beta}{(1+(1-\beta)z)(1-(1-\beta)z)},$$

$$\min_{|z|\le 1}|f'(z)| = |f'(\pm i)| = \frac{1-\beta}{2(1-\beta)+\beta^2} \to \frac{1}{2},$$

$$|f(\pm 1)| = l \sim -\frac{1}{2}\log\beta \quad \text{and} \quad \alpha \sim \frac{\pi}{4l},$$

$$\|f'\|_\infty = |f'(\pm 1)| = \frac{1-\beta}{(2-\beta)\beta} \sim \frac{1}{2\beta} \sim \frac{1}{2}e^{2l}.$$

Also, note that

$$\|f - f_N\|_\infty \le \frac{R^{-(N+2)}}{N}\sum_{k=0}^{\infty}R^{-2k} = \frac{R^{-N}}{N(R^2-1)}.$$

In our computations, we have used a parametrization of the boundary, $(1+r^2)\cos y = (1-r^2)\cosh x$, where $r = 1-\beta$, provided by John Pfaltzgraff (private communication). Also, we have normalized the curves so that $|f(\pm 1)| = 1$ and $|f(\pm i)| = \alpha$. A choice of β then gives an α. One could, of course, solve for β for a given α, but we have not done this. Again $C = .01$ gives a reasonble fit to the data in Fig. 8. This map is perhaps the simplest example of the severe distortions, seen as the *crowding* of points mapped near ± 1 by f^{-1}, which occurs for maps from the disk to slender regions. As is typical in such cases, the distortions vary exponentially with the aspect ratio $\sim 4l/\pi$ of the region. Note that for z near ± 1 the series starts to grow like the harmonic series as $R \downarrow 1$.

(v) *Ellipse*; see Fig. 9. Here $\Gamma : \gamma(\sigma) = \rho(\sigma)e^{i\sigma}$, where $\rho(\sigma) = \alpha/\sqrt{1-(1-\alpha^2)\cos^2\sigma}$ for $0 \le \sigma \le 2\pi$ and $0 < \alpha \le 1$. The exact map is given in [34] in terms of an elliptic integral:

$$f(z) = \sqrt{1-\alpha^2}\sin\frac{\pi}{2K}\int_0^{z/\sqrt{k}}\frac{dt}{\sqrt{(1-t^2)(1-k^2t^2)}}.$$

In [55] Zemach discusses the crowding for this map and finds

$$\|f'\|_\infty = |f'(\pm 1)| \sim \frac{\alpha^2}{2\pi}e^{\pi^2/4\alpha}.$$

The map $w = f(z)$ can be computed by composing a sequence of known maps. Here we give a modification of the construction in [32, pp. 295–296]. Our construction uses the Schwarz–Christoffel transformation between the rectangle and the disk instead of the half plane, so that SCPACK [47] may be employed. First, map the upper half of the unit disk, $|z| \le 1, \operatorname{Im} z \ge 0$, to the right half of the unit disk in the ξ-plane with the semicircle mapping to the diameter $[i, -i]$, by $\xi(z) = (i-z)/(i+z)$. Next, use SCPACK to compute the Schwarz–Christoffel map $\zeta = \zeta(\xi)$ from the full unit disk

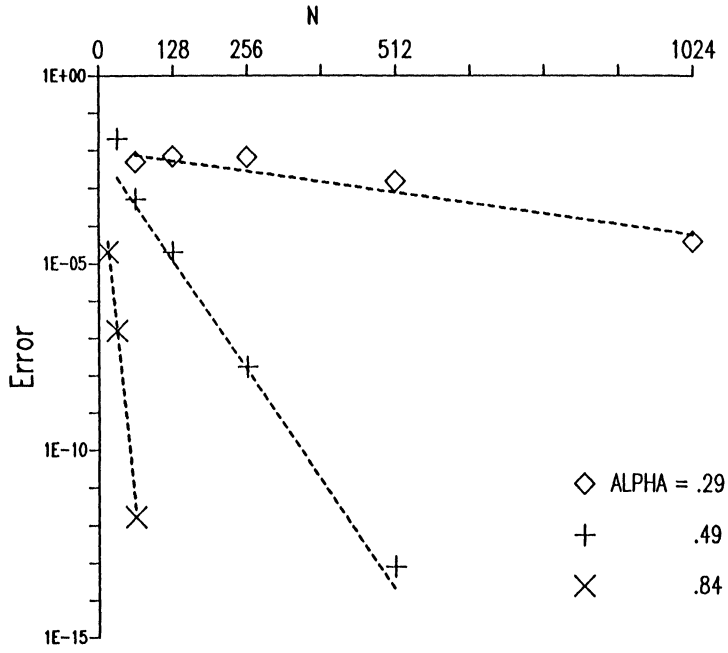

FIG. 8. *Discretization errors for Wegmann's method for* arctanh *regions.*

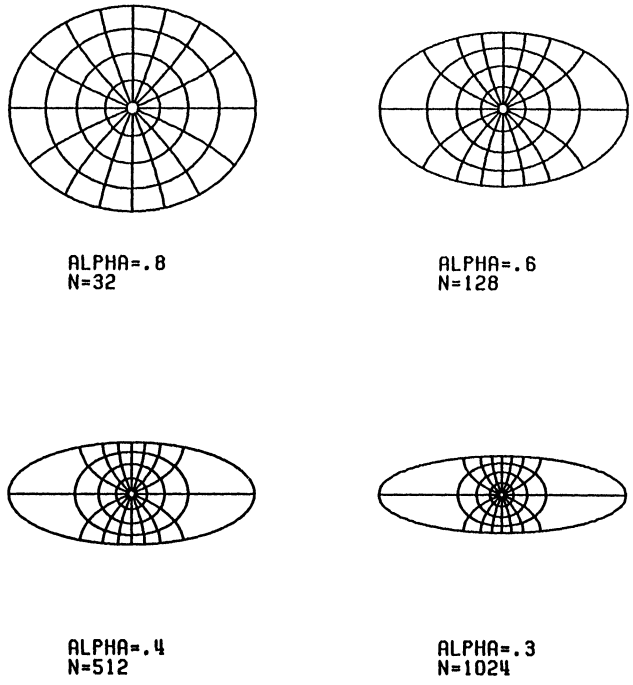

FIG. 9. *Ellipses with Wegmann's method.*

$|\xi| \leq 1$ to the rectangle in the ζ-plane with base $[-\pi/2, \pi/2]$ and height $i2\log\rho$, and normalized such that $\zeta(0) = i\log\rho$ and $\zeta(1) = 0$. Finally, the rectangle is mapped to the upper half of an ellipse in the w-plane by $w(\zeta) = \sin\zeta$. The line segment $\operatorname{Im}\zeta = \log\rho$ bisecting the rectangle will map to an ellipse in the w-plane with major axis $(\rho + 1/\rho)/2$, minor axis $i(\rho - 1/\rho)/2$, and focii ± 1. The map $w = h(z) = \sin\zeta(\xi(z))$ from the full disk $|z| \leq 1$ to the full ellipse is gotten by reflecting through the real axis. The desired α is given by $\alpha = (\rho^2 - 1)/(\rho^2 + 1)$ and our normalized ellipse map with $f(1) = 1$ and $f(i) = i\alpha$ is given by $f(z) = \sqrt{1-\alpha^2}\, h(z)$.

We can now further analyze the asymptotic behavior of the ellipse map as $\alpha \downarrow 0$. Let $h(\pm 1/R) = \pm 1$, where ± 1 are the focii of the (unnormalized) ellipse and $R > 1$. Then it can be seen from the above construction that the singularities of h nearest to the unit disk are branch points of the square root at $\pm R$. The preimages of the corners in the Schwarz–Christoffel map are $\pm\xi(1/R)$ and $\pm\xi(R)$. Let $\theta = \arg(\xi(R)/\xi(1/R))$. A slight modification of the discussion of crowding for the Schwarz–Christoffel map given in §3(i) below shows that

$$\theta \sim 8e^{-\pi^2/4\log\rho} \text{ as } \rho \downarrow 1,$$

and so

$$R \sim 1 + 4e^{-\pi^2/4\alpha} \text{ as } \alpha \downarrow 0.$$

Table 1 compares some calculated values of R with the asymptotic estimates for various α.

TABLE 1

α	R	$1 + 4e^{-\pi^2/4\alpha}$
.8	1.53	1.18
.6	1.12	1.06
.4	1.011	1.008
.3	1.0013	1.0010

Using the calculation of the exact map given above, we see in Fig. 10 that $\|f - \tilde{f}_N\|_\infty \approx CR^{-N/2}$ for Wegmann's method with $C = .01$. This is another example of a slender region that crowds. Numerical experiments in [4], [8], and [22] show how difficult it is to produce this map or, equivalently, the map to the exterior of an inverted ellipse for even moderate $\alpha \approx .2$. The similarity of the data in Figs. 8 and 10 should be noted.

We may summarize the relation between the singularities and the maximum derivatives in Table 2:

TABLE 2

Region	$R = 1 + \delta(\alpha)$	$\|f'\|_\infty = \frac{1}{O(\delta(\alpha))}$
Circle	$1 + \alpha + O(\alpha^2)$	$\frac{2}{\alpha} + 1$
Inverted ellipse	$1 + \alpha + O(\alpha^2)$	$\frac{1}{\alpha}$
Cassini oval	$1 + \alpha^2 + O(\alpha^4)$	$\frac{1}{2\alpha^2} + \frac{1}{2}$
Arctanh	$\sim 1 + O(e^{-\pi/2\alpha})$	$\sim \frac{1}{2}e^{\pi/2\alpha}$
Ellipse	$\sim 1 + 4e^{-\pi^2/4\alpha}$	$\sim \frac{\alpha^2}{2\pi}e^{\pi^2/4\alpha}$

So for the above examples we have roughly $R = 1 + 1/O(\|f'\|_\infty)$ and

$$\|f - f_N\|_\infty \leq CR^{-N} = Ce^{-N\log R} \approx Ce^{-N/\|f'\|_\infty}.$$

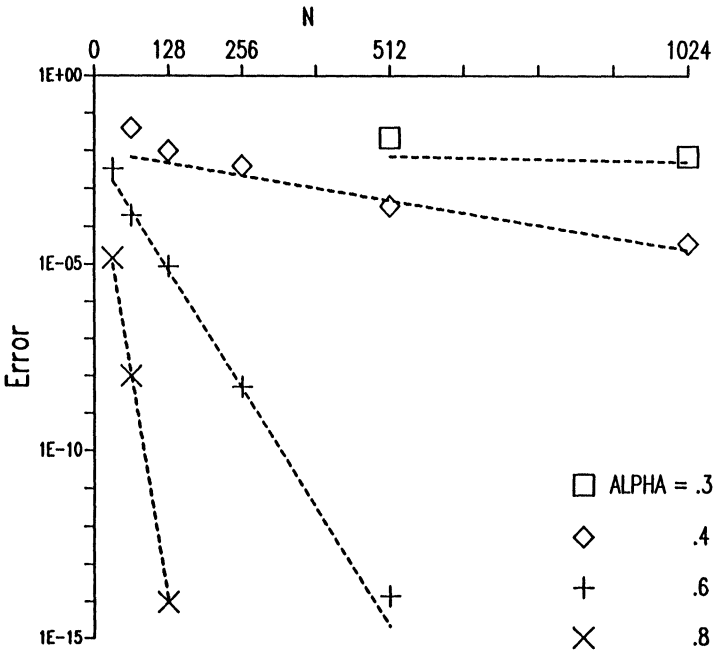

FIG. 10. *Discretization errors for Wegmann's method for ellipses.*

This is *Zemach's rule* for the above analytic curves. For the ellipse map where R is a branch point, it is easy to show that $\max_{|z|\le R}|f(z)| = (\rho^4+1)/(\rho^3+\rho) \to 1$ as $\rho \downarrow 1$. Cauchy's estimate then gives the $O(R^{-N})$ behavior of the error for the truncated series. For families of analytic curves for which $f(z)$ becomes unbounded as z approaches R, application of Cauchy's estimate is less straightforward. This is illustrated in the following theorem. Obtaining precise information on the singularities of f may require the use of asymptotic techniques such as those in [3, pp. 255–257].

THEOREM 3. *For a family of analytic curves* $\Gamma : \gamma_\alpha(\sigma)$ *with* $R = 1+\delta(\alpha)$ *and for* r *fixed,* $0 < r < 1$ *and* $R_r = 1 + r\delta(\alpha)$ *we have*

$$\|f - f_N\|_\infty \le C_{\alpha,r} R_r^{-N}.$$

Proof. For $|z| \le R_r = 1 + r\delta(\alpha)$, there is an M_r such that $|f(z)| \le M_r$. Cauchy's estimate gives $|a_k| \le M_r R_r^{-k}$. Therefore, for $|z| \le 1$,

$$\|f - f_N\|_\infty \le \sum_{k=N+1}^{\infty} |a_k| \le M_r \frac{R_r^{-N}}{R_r - 1} \le \frac{M_r}{r\delta(\alpha)} R_r^{-N}. \qquad \square$$

Similarly, we can estimate the error in the interior of an analytic curve if the a_k's are known accurately: Let $|z| = r < 1$. Then for our curves normalized so that $\|f\|_\infty = 1$, the Cauchy estimate gives $|a_k| \le 1$. Therefore,

$$|f(z) - f_N(z)| \le \Big|\sum_{k=N+1}^{\infty} a_k z^k\Big| < \sum_{k=N+1}^{\infty} r^k = \frac{r^{N+1}}{1-r}.$$

For example, $N = 10$ and $r = \frac{1}{2}$ gives an error of less than 10^{-3}, so the map may be evaluated accurately in the interior of the unit disk with only a few accurate coefficients

and may look reasonable even when the solution is quite poor.

3. Crowding estimates. In this section we review several estimates for crowding. In (i) we consider the case of the Schwarz–Christoffel transformation to rectangles of large aspect ratio. In (ii) we apply estimates of Gaier based on the curvature of the boundary and show that they do not capture the severe crowding phenomenon. In (iii) we discuss Zemach's estimates based on the Menikoff–Zemach integral equation for the boundary correspondence. In (iv) we give a brief review of Dubiner's general theory. In (v) we apply a theorem of Pfluger from the theory of conformal invariants to give a general estimate of the crowding for elongated sections of a region. In (vi) we give an example which exhibits the algebraic crowding for pinched regions. In (vii) we briefly discuss Wegmann's estimates of $|f'|$. Finally, in (viii) we mention the recent related work on domain decomposition methods for computing conformal modules.

(i) *Schwarz–Christoffel transformation.* Let f be the Schwarz–Christoffel transformation for the upper half plane to the rectangle with corners $\pm K, \pm K + iK'$. Using symmetry we fix $f(\pm 1) = \pm K, f(\pm 1/k) = \pm K + iK'$, and we also have $f(0) = 0$ and $f(i/\sqrt{k}) = iK'/2$, where $0 < k < 1$. Then

$$f(w) = \int_0^w \frac{d\tau}{\sqrt{1-\tau^2}\sqrt{1-k^2\tau^2}}.$$

We map the upper half plane to the unit disk by

$$z(w) = \frac{i - \sqrt{k}w}{i + \sqrt{k}w}.$$

Then $z(0) = 1, z(\infty) = -1, z(\pm 1) = e^{\pm i\theta/2}$, and $z(-_+ 1/k) = -e^{\pm i\theta/2}$, where

$$\theta = \arg \frac{z(1)}{z(-1)} = 4 \arctan \sqrt{k}.$$

We now want to ask what happens to θ as the aspect ratio $K'/2K$ becomes large (as $k \downarrow 0$). In this case we have

$$\theta \approx 4\sqrt{k},$$

$$K = \int_0^1 \frac{d\tau}{\sqrt{1-\tau^2}\sqrt{1-k^2\tau^2}} \to \int_0^1 \frac{d\tau}{\sqrt{1-\tau^2}} = \frac{\pi}{2},$$

and

$$K' = \int_1^{1/k} \frac{d\tau}{\sqrt{1-\tau^2}\sqrt{1-k^2\tau^2}} \sim \log \frac{4}{k}.$$

The behavior of K' is derived in [54, p. 522], using elementary estimates of the integrals. Putting these together, we get

$$k \sim 4e^{-\frac{\pi K'}{2K}}$$

and finally

$$\theta \sim 8e^{-\frac{\pi K'}{4K}}.$$

Thus, for the conformal map from the unit disk to a rectangle of large aspect ratio, the crowding of the preimages of the corners can be severe. The estimates above are also discussed in [28] and [36], with standard references to the elliptic function literature. We wish to point out the easy estimate in [54]. For a comparison of the maps to four rectangles of increasing aspect ratios, see Fig. 3 in [28].

Note that it is the global property of aspect ratio that is causing the crowding and not the local effects of the corners. Acute corners are singularities in f' which magnify infinitesimal regions infinitely. By contrast, the crowding in example (iv), §2, for instance, is caused by a singularity of f near which f becomes unbounded. Similarly, it is not the curvature which is causing trouble, as the following estimates of Gaier indicate.

(ii) *Gaier's estimates.* In [16] and [25] various equations for $t(\sigma)$, the boundary correspondence for the map to the disk, are discussed. In particular, equations for $t'(\sigma)$ would seem right for estimating the distortions in the map. Two such equations derived in [16] and [25] are the equation of *Warschawski,*

$$t'(\sigma) + \int_0^L N(\tilde{\sigma}, \sigma) t'(\tilde{\sigma}) d\tilde{\sigma} = 2\mathrm{Im}\frac{\gamma'(\sigma)}{\gamma(\sigma)},$$

for the map from the interior of $\gamma(\sigma)$, and the equation of *Banin,*

$$t'(\sigma) = \int_0^L N(\tilde{\sigma}, \sigma) t'(\tilde{\sigma}) d\tilde{\sigma},$$

for the map from the exterior of $\gamma(\sigma)$, where

$$N(\tilde{\sigma}, \sigma) = \frac{1}{\pi}\mathrm{Im}\frac{\gamma'(\sigma)}{\gamma(\sigma) - \gamma(\tilde{\sigma})}$$

is the *Neumann kernel.* For smooth convex curves with maximum and minimum radii of curvature $\rho_{\max}$ and $\rho_{\min}$, respectively, Gaier proves the following theorems.

THEOREM 4 [16, Thm. 4.2, p. 45].

$$\frac{1}{2\pi\rho_{\max}} \leq N(\tilde{\sigma}, \sigma) \leq \frac{1}{2\pi\rho_{\min}}.$$

Applying this estimate to the above equations for $t'(\sigma)$, gives the following.

THEOREM 5 [16, Thm. 4.3, p. 46]. *For the interior map*

$$0 < t'(\sigma) \leq \frac{2}{\alpha} - \frac{1}{\rho_{\max}},$$

and for the exterior map

$$\frac{1}{\rho_{\max}} \leq t'(\sigma) \leq \frac{1}{\rho_{\min}}.$$

Note that these estimates do not capture the crowding, since the lower estimate for the interior map would have to be exponential in α. (The lower estimate is just the fact that $t(\sigma)$ is increasing. It is included only for emphasis.) The reason for this would seem to be that these estimates are based on the Neumann kernel, which is closely related to the curvature, and curvature, like a corner, is a local property of the the curve. These estimates are not necessarily sharp for some of our families of test curves. For instance, let us consider some cases where the bounds are converted to bounds on $\sigma'(t)$. For the map to the interior of the family of circles in example (i), we have $\alpha/(2-\alpha) \leq \sigma'(t) \leq (2-\alpha)/\alpha$. Gaier's estimate gives $\alpha/(2-\alpha) \leq \sigma'(t) < \infty$. Note that the lower bound is sharp for this family. For the family of ellipses in example (v), we have $\rho_{\max} = 1/\alpha^2$ and $\rho_{\min} = \alpha$. The exact map for the interior gives $|f'(\pm i)| \leq \sigma'(t) \leq |f'(\pm 1)| \approx (\alpha^2/2\pi)e^{\pi^2/2\alpha}$. Gaier's bounds in this

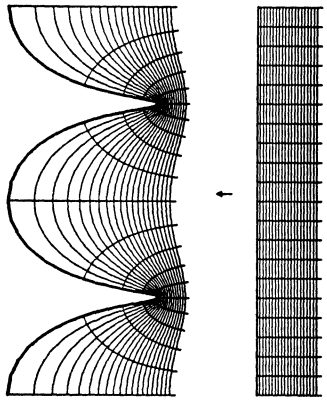

FIG. 11. *Crowding for map of half plane,* Re $z \geq .2$ *by* $f(z) = 2 \log \sinh z/2$.

case give $\alpha/(2-\alpha^3) \leq \sigma'(t) \leq \infty$, so the exponential behavior of the upper bound is not captured at all. The exact (Joukowski) map to the exterior of the ellipse gives $1 \leq \sigma'(t) \leq 1/\alpha$, whereas Gaier's bounds give $\alpha \leq \sigma'(t) \leq 1/\alpha^2$. Though these bounds are not sharp they do demonstrate that the map to the exterior of a slender region is not a difficult case. This is seen in the numerical experiments in [8] and [24] and in aeronautical engineering applications where Fourier series methods are used to compute potential flow over the exterior of often slender airfoils. The difficult exterior case is the map to, say, the exterior of an inverted ellipse. Roughly speaking, whenever "fingering" occurs in the target region, the mapping problem will be ill conditioned; see Fig. 11. Note that Gaier's estimate can be used for the interior of the nonconvex inverted ellipse. There the exact map of example (ii) gives $\alpha^2 \leq \sigma'(t) \leq 1/\alpha$. Using Gaier's bounds for the exterior of an ellipse and reflecting gives $\alpha^3 \leq \sigma'(t) \leq 1/\alpha^3$.

(iii) *Zemach's estimates.* Consider the map from the vertical strip $-\pi \leq u \leq \pi, v \geq 0$ in the $w = u + iv$-plane to the strip $-\pi \leq x \leq \pi, y \geq y(x)$, in the $z = x + iy$-plane, where $y(x)$ is a given 2π-periodic function. Let $z = z(w)$ be the conformal map between the strips for which $z(\pm\pi) = \pm\pi + iy(\pm\pi)$ and the vertical sides map to the vertcal sides. Then $z(w)$ will be determined if $u = u(x)$ is found for $-\pi \leq x, u \leq \pi$. In [31], $u = u(x)$ is found as a solution to the *Menikoff–Zemach equation,*

$$y(x) = y_0 + 2\log 2 + \frac{1}{\pi}\int_{-\pi}^{\pi} \log\left|\sin\frac{1}{2}(u(x) - u(x'))\right| dx'.$$

Similar equations can be derived for other geometries, such as the map between the unit disk and the interior of a closed curve. As illustrated in Fig. 11, the maximum and minimum crowding will take place where $dy/dx = 0$. In [55], Zemach assumes severe crowding, $du/dx \ll 1$, near $x = 0, u(0) = 0$ for $y(0)$, a minimum, and derives an estimate for the local behavior of $u(x)$. He applies these estimates to some examples. For an ellipse in circular geometry he gets the correct asymptotic behavior within a constant factor. For the cosine curve, $y(x) = -\frac{1}{\alpha}\cos x$, he finds

$$\frac{du}{dx}(0) \sim \frac{2\pi}{\alpha} e^{-\pi/2\alpha \int_0^\pi \sin x/x dx}.$$

He also gets an estimate for the minimum crowding:

$$\frac{du}{dx}(\pm\pi) = \sqrt{\frac{2}{\alpha}}.$$

A similar example is given in the next paragraph; see Fig. 11.

(iv) *Dubiner's work.* We give here some brief remarks on the results that Dubiner presented in his Ph.D thesis [12]. Unfortunately, to this author's knowledge, this work has never been published in an accessible form. Dubiner shows quite generally that the conformal map f from the disk to a region may have $\max|f'|$ very large, growing exponentially with the aspect ratio for slender regions. However, $\log|f'|$ is well-behaved and $\min|f'|$ is reasonable. His estimates exploit the theory of conformal invariants, extremal length, and harmonic measure. The key estimate of f' for the severe crowding uses the arctanh function in §2, example (iv). In an introductory example, Dubiner uses the following map, which illustrates the crowding for the half plane mapped to a half plane with "fingering." Such geometries may occur in computations of surface waves [30] and the Rayleigh–Taylor instability [31]. The map is $f(z) = 2\log\sinh z/2$ from the right half plane to the slit plane as shown in Fig. 11. Curves $x = c > 0, c$ constant, map to finger-like curves as $c \downarrow 0$. Note in this case that $f'(x + i\pi) \downarrow 0, f(x) \sim 2\log x$, and $f'(x) \sim 1/x$ as $c \downarrow 0$. If we take $\alpha := -1/\log x$ as the aspect ratio, then we see again $f'(x) \sim e^{1/\alpha}$. Dubiner applies this example to the region $x \geq -\frac{1}{\alpha}\cos y$ to get the same estimates for the maximum and minimum derivatives as those reported above due to Zemach.

Besides attempting to give bounds for $|f'|$, another way to study the distortions in f is to try to estimate the harmonic measure of a boundary arc at an interior point of the region. Dubiner also gives such estimates in terms of conformal invariants such as extremal distance. We give a similar result next. Dubiner's other results include a perturbation formula connecting perturbations of the boundary to perturbations of the map. A numerical method is also suggested, but no experiments are reported.

(v) *Pfluger's Theorem.* In this section we use some results from the theory of conformal invariants [1] to estimate the crowding.

For an arc E on the boundary Γ of Ω, we recall the following definition.

DEFINITION 1. *The harmonic measure of E with respect to Ω, $\omega(w) = \omega(w, E, \Omega)$, is the unique bounded harmonic function on Ω with boundary values 1 at interior points of E and 0 at interior points of $\Gamma - E$.*

If $w = f(z)$ maps D conformally onto the Jordan domain Ω and $g = f^{-1}$, then

$$\omega(z, f^{-1}(E), D) = \omega(f(z), E, \Omega),$$

since harmonic functions are preserved by conformal maps. The boundary arc E maps to an arc $f^{-1}(E)$ on the unit circle. It is a familiar consequence of the mean value property of harmonic functions that

$$\text{meas}(f^{-1}(E)) = 2\pi\omega(0, f^{-1}(E), D) = 2\pi\omega(f(0), E, \Omega),$$

where meas denotes linear measure on the unit circle. Thus, estimates of the harmonic measure $\omega(f(0), E, \Omega)$ can be used to assess the distortion of the boundary set E under conformal mapping by f.

Next, we recall the notion of extremal distance between two disjoint sets E' and E in the closure of Ω. We consider the family of Riemannian metrics $ds = \rho|dz|$ which includes the Euclidean metric.

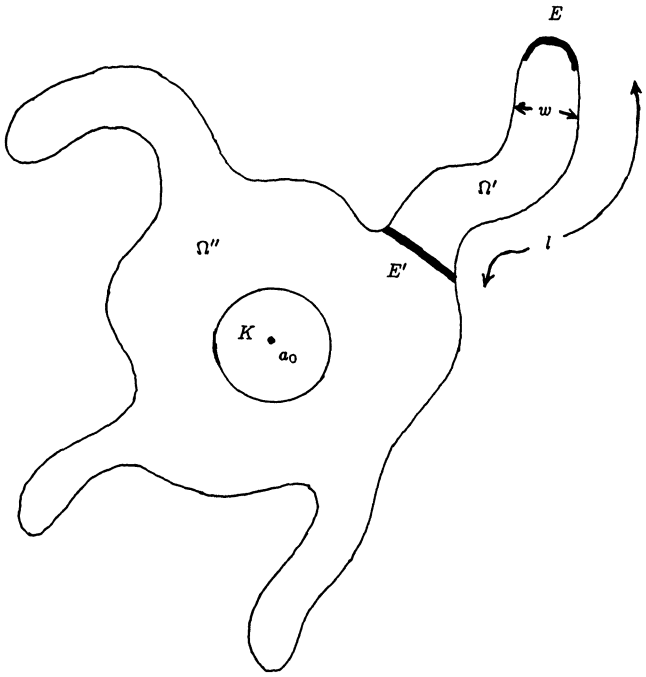

FIG. 12. *Region with elongated section for Pfluger's theorem.*

DEFINITION 2. *The extremal distance between E' and E is*

$$\lambda(E', E, \Omega) = \sup_{\rho} \frac{(\inf_{\gamma} \int_{\gamma} \rho |dz|)^2}{\int\int_{\Omega} \rho^2 dx dy},$$

where the supremum is over all nonnegative, Borel measurable $\rho = \rho(x, y)$ such that $0 < \int\int_{\Omega} \rho^2 dx dy < \infty$, and the infimum is over all locally rectifiable arcs γ in Ω connecting E' and E.

Under a conformal map f the metric ρ will transform as $ds = \rho|dz| = \rho'|df|$, where $\rho' = \rho/|f'|$. Thus, we see that extremal distance is a *conformal invariant*, which may be thought of as *length*^{2}*/area*. If Ω is a rectangle of length l and width w and E' and E are opposite sides of Ω a distance l apart, then $\lambda(E', E, \Omega) = l/w$. That is, the extremal distance is just the *conformal module* of the rectangle. Similarly, in [6] it was noted that for a "slender" region Ω of length l and width w with E' and E at the "ends" we have $l \gg w$ and the area of $\Omega \approx lw$. Then an inequality due to Rengel [29, p. 22] gives $\lambda(E', E, \Omega) \approx l/w$. Mapping Ω to a rectangle and applying the estimates for the Schwarz–Christoffel transformation in (i) will then yield the crowding estimate.

There is, however, a more precise and general estimate of harmonic measure in terms of extremal distance due to Pfluger. Let E be a set on the boundary of $\Omega = \Omega' \cup \Omega'' \cup E'$. Fix $a_0 \in \Omega$ and a small compact set K in Ω containing a_0, as in Fig. 12. Then Pfluger's theorem says

$$\omega(a_0, E, \Omega) \leq Ce^{-\pi\lambda(K,E,\Omega)},$$

where the constant C depends only on a_0 and K and does not depend on the boundary set, E. If E is a boundary arc at the end of a long "finger" Ω' of length l and width

w protruding from Ω and $K \subset \Omega''$ as in Fig. 12, then as was observed in [11],

$$\lambda(K, E, \Omega) \geq \lambda(E', E, \Omega') \geq l/w(1+\epsilon),$$

where the area of $\Omega' = lw(1+\epsilon)$. Combining this with Pfluger's inequality and adjusting the constant yields the crowding estimate,

$$\omega(a_0, E, \Omega) \leq C' e^{-\pi l/w}.$$

To apply this to a rectangle of length l and width w and a_0 at the center of the rectangle, we must replace l by $l/2$ in the estimate. This example shows that the estimate is sharp.

In [44, §§9.4 and 9.5], we have essentially this same crowding estimate along with a proof of Pfluger's theorem.

For a slender region the crowding estimate may be thought of as a simple caricature of *Saint Venant's Principle* from the theory of elasticity, expressing the exponential decay-of-influence of boundary data at E on the value of a harmonic function at a_0 as a function of the distance from a_0 to E; see, e.g., [26] and the references there for a lead into the extensive literature in this area.

(vi) *Algebraic crowding.* In examples (i), (ii), and (iii) of §2 where the target regions are pinched, we saw that the maximum derivatives of f behaved like $O(\alpha^{-k})$, in contrast to the exponential behavior for elongated regions. Here we present a simple example which displays this algebraic behavior more generally. For $0 < \alpha < 1$, and $0 < s \leq \pi$ consider the bowtie-shaped region Ω interior to the boundary formed by an arc E given by $e^{i\theta}, -s/2 \leq \theta \leq s/2$, the line segment from $e^{is/2}$ to $\alpha e^{is/2}$, the arc given by $\alpha e^{i\theta}, s/2 \leq \theta \leq \pi - s/2$, the line segment from $\alpha e^{i(\pi - s/2)}$ to $e^{i(\pi - s/2)}$ and the reflection of these curves through the origin. This gearlike domain is our model of a pinched region of thinness α. If we map this region into the upper half plane by the function $-i \log z$, the boundary will map to a periodic step function, with the bow mapping to a step of width $w = s$ and height $l = -\log \alpha$. If we then map this region conformally to the upper half ζ-plane with points $k\pi$ going to $k\pi$, then the base of the steps of length s will map to intervals on the x-axis of length θ. A crowding estimate given in [14] shows that

$$\theta \leq C e^{-\pi l/w} = C\alpha^{\pi/s}.$$

If we map the upper half ζ-plane to the disk with the function $e^{i\zeta}$, then $\omega(0, E, \Omega) = \theta$ and the estimate gives the algebraic crowding of the image of E on the disk as $\alpha \downarrow 0$.

We could change this example slightly to treat the map from the disk slit from 1 to α to the full disk with 0 going to 0. If we take E to be the unit circle and $s = 2\pi$, our estimate gives

$$\omega(0, E, \Omega) \leq C\sqrt{\alpha}.$$

This example is discussed in [11, ex. 5.3] and represents a limiting case for algebraic crowding.

(vii) *Wegmann's estimates.* Wegmann [52], [53] also gives estimates of the crowding. He gives a lower bound for the supremum norm of the derivative of the map from the disk to an elongated region by combining the known behavior of certain explicit maps with a generalization of the Schwarz lemma. His results are somewhat less general than the results above in that his regions must be contained in a smallest rectangle of length l and width w. However, he does give a detailed discussion of the constant C for certain regions and shows which elongated regions will produce minimal crowding.

(viii) *Domain decomposition methods.* Papamichael and Stylianopolis [35], [38]–[42] have also recently proposed a domain decomposition procedure for computing the map from a rectangle to an elongated strip. The strip is decomposed into shorter strips. Due to the effects of the crowding, the sum of the conformal modules of the shorter strips is often a good approximation to the module of the full strip. Related work by Gaier and Hayman concerning crowding and the computation of conformal modules for long quadrilaterals is reported in [19] and [20].

4. Remarks on solving boundary value problems. We now discuss briefly the effect of crowding on a boundary value problem conformally transplanted to the unit disk; see also [7]. Suppose we want to solve the Laplace equation, $\Delta u = 0$, in the region Ω given by the image of the unit disk under the normalized map in §2 (iv), $f(z) = \operatorname{arctanh}(1-\beta)z/\operatorname{arctanh}(1-\beta)$ with $u = y$ on the boundary. Then, of course, $u = \operatorname{Im} f(z)$. Also, $\alpha = |f(\pm i)|$. In Fig. 13 a, b, and c for $\beta = .5, .1, .01$, we show the regions, the boundary correspondence $\sigma(t)$, where σ is arclength, the boundary data $u(\sigma) = y$ plotted against σ, and the transplanted boundary data $u(\sigma(t)) = y$ plotted against t.

The effect of the crowding on the transplanted data is to make the data more like a step function, which has a slowly converging Fourier series. We illustrate the problems this may cause for computations as follows: The solution to our Dirichlet problem in the disk $0 < r < 1$ is

$$u(re^{it}) = \sum_{n=-\infty}^{\infty} A_n r^{|n|} e^{int},$$

where A_n are the Fourier coefficients of $u(\sigma(t)) = \operatorname{Im} f(e^{it})$ with $A_n = \overline{A}_n$ and $A_n = a_n + ib_n$. Suppose we wish to find the Dirichlet integral $D[u]$ of u in the original region Ω in the w-plane. Since $D[u]$ is preserved under conformal mapping we have

$$D[u] = \iint_{\Omega} |\nabla_w u(w)|^2 = \iint_{D} |\nabla_z u(f(z))|^2 = 4\pi \sum_{n=1}^{\infty} n(a_n^2 + b_n^2).$$

From §2 (iv) we see $b_{2k-1} = (1-\beta)^{2k-1}/((2-4k)\operatorname{arctanh}(1-\beta))$ for $k = 1, 2, \ldots$ and $a_n, b_n = 0$, otherwise. For small α (β near 1) this is a slowly converging series. If we use an $N = 2^M$-point FFT to find the discrete Fourier coefficients of $u(\sigma(t))$ and then to estimate $D[u]$, we get the results in Table 3. N_e in the table is the first $N = 2^M$ such that $D[u]$ is computed to 10^{-2} accuracy. The rapid increase of N_e with aspect ratio clearly shows the effects of crowding. With β near 0, the initial Fourier coefficients are roughly $O(n^{-1})$, like those for a step function. It might be wondered whether use of filtering, acceleration of convergence, or perhaps, wavelets [2] might help here.

TABLE 3

β	α	$D[u]$	N_e	$\|f'(\pm 1)\|$
.5	.84	2.65	16	.67
.1	.47	1.63	64	4.7
.01	.29	1.03	512	49.7
.001	.20	.75	4096	499.7

5. Remarks on other methods. One way to handle the crowding problem is to try to avoid it by choosing a computational domain more suited to the target region. Recently Howell and Trefethen [28] proposed a Schwarz–Christoffel method for

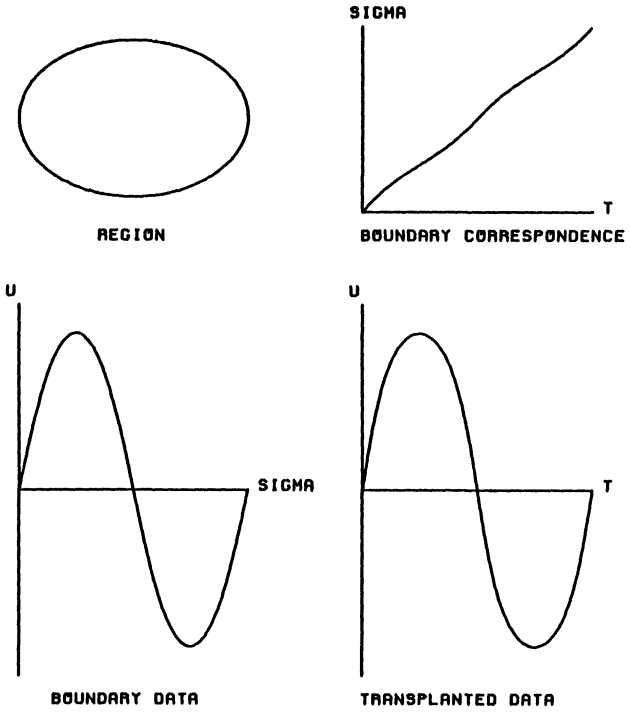

FIG. 13a. *The effect of crowding on transplanted boundary data,* $\beta = .5$.

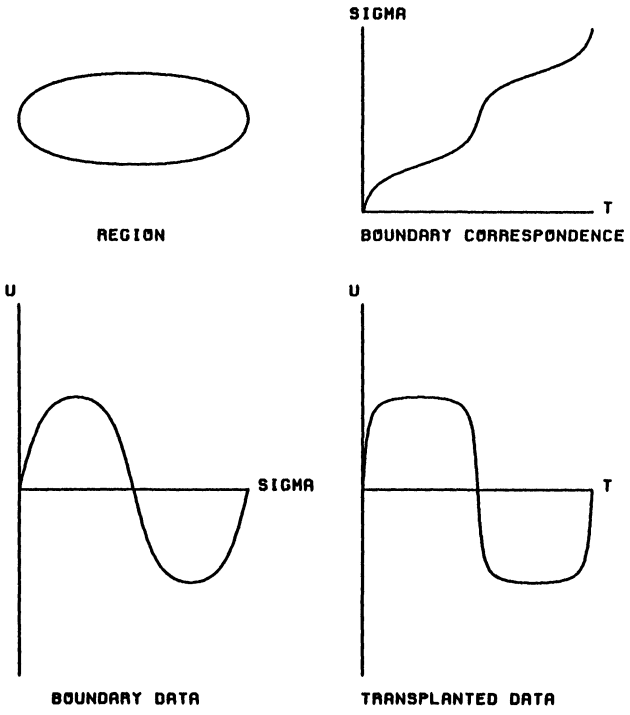

FIG. 13b. *The effect of crowding on transplanted boundary data,* $\beta = .1$.

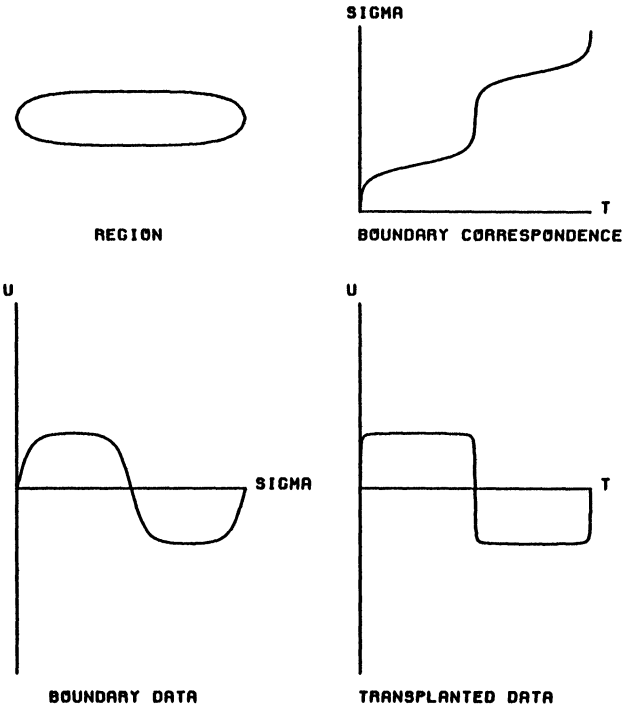

FIG. 13c. *The effect of crowding on transplanted boundary data,* $\beta = .01$.

elongated polygons which uses the infinite strip as a computational region instead of the disk or half plane. The map between elongated rectangles and elongated polygons of the same aspect ratio (conformal module) can then be found. Maps from doubly connected regions to annular regions seem to suffer less from severe distortions. Thus, Papamichael, Kokkinos, and Warby [36] proposed a method for mapping slender, simply connected regions with enough symmetry to allow them to be pieced together to form a doubly connected region. The region is then mapped to an annulus and the annulus to a strip. The map of the original region to a rectangular portion of the strip is then available. In [13] and [14], Floryan and Zemach have derived generalized Schwarz–Christoffel transformations which may provide more suitable choices for computational domains. However, for any computational domain a severe target region can be found. For instance, Howell and Trefethen's strip map would not be appropriate for a T-shaped region.

In [9] Elcrat and the author give a Fornberg-like method which uses the ellipse as the computational domain. The map from an ellipse to a slender target region of similar aspect ratio can then be computed with a moderate number of mesh points. The method is based on approximating the Chebyshev series of the map and uses fast Fourier transform methods. It has been generalized further by Elcrat, Pfaltzgraff, and the author in [10] to employ a cross-shaped region as the computational domain. The map is then approximated by the Faber series for the cross-shaped domain. In both the ellipse and the cross case the Dirichlet problem for the Laplace equation can be transplanted to the computational domain and its solution represented efficiently by a Faber series. The effects of §4 can then be avoided in certain cases. Further generalizations of these methods should be possible.

Explicit maps such as those due to Grassmann [21] may be used to map extreme regions to nearly circular regions. A Fourier series map to the nearly circular region can then be easily computed and composed with the inverted explicit maps to form a map to the original region. However, experiments reported in [4] and [7] indicate that this does not circumvent the crowding problem since the large distortions in the explicit maps magnify errors in the Fourier series map.

Maps from the region to the disk suffer less severely from crowding; see [27] and [33]. The effect of the curve geometry on the accuracy of the method in this case requires further study. According to [12] the stretching is less severe than the crowding. For maps to the disk we discretize in the plane of the boundary curve. Sufficient accuracy would seem to require that the images of these points sufficiently "resolve" the boundary of the disk. Thus, curves which cause the most stretching would present the greatest difficulties. This is indicated, for instance, in Trummer's [48] experiments with the Kerzman–Trummer method for maps from the inverted ellipse and the Cassini oval to the disk. The stretching for these regions is $O(\alpha^{-2})$ and $O(\alpha^{-1})$, respectively, as is given by $|f'(\pm i)|^{-1}$ in §§2 (ii) and (iii). This roughly predicts the discretization error, though estimates like those in §2 are not at hand. (Our α is equal to $\sqrt{(1-\alpha^2)/(1+\alpha^2)}$ for Trummer's α for Cassini ovals.) In [43] the singularities near the boundary are used to improve maps to the disk. One might wonder whether similar techniques can be used for maps to the region, in particular, for regions with severe crowding.

Acknowledgments. Much of this work grew out of the author's Ph.D thesis [4]. The author thanks Olof Widlund, Nick Trefethen, John Pfaltzgraff, Alan Elcrat, and Rudolf Wegmann for their interest in various stages of this work and Dale Pullin for pointing out reference [3].

REFERENCES

[1] L. AHLFORS, *Conformal Invariants*, McGraw-Hill, New York, 1973.

[2] G. BEYLKIN, R. COIFMAN, AND V. ROKHLIN, *Fast wavelet transforms and numerical algorithms* I, Comm. Pure Appl. Math., 44 (1991), pp. 141–183.

[3] G. F. CARRIER, M. KROOK, AND C. E. PEARSON, *Functions of a Complex Variable: Theory and Technique*, McGraw-Hill, New York, 1966.

[4] T. K. DELILLO, *A comparison of some numerical conformal mapping methods*, Ph.D thesis, New York University, New York, 1985.

[5] ———, *On some relations among numerical conformal mapping methods*, J. Comput. Appl. Math., 19 (1987), pp. 363–377.

[6] ———, *A note on Rengel's inequality and the crowding phenomenon in conformal mapping*, Appl. Math. Lett., 3 (1990), pp. 25–27.

[7] ———, *On the use of numerical conformal mapping methods in solving boundary value problems for the Laplace equation*, in Advances in Computer Methods for Partial Differential Equations-VII, R. Vichnevetsky, D. Knight, and G. Richter, eds., Seventh IMACS Symposium Proceedings, Rutgers University, New Brunswick, NJ, 1992, pp. 190–194.

[8] T. K. DELILLO AND A. R. ELCRAT, *A comparison of some numerical conformal mapping methods for exterior regions*, SIAM J. Sci. Statist. Comput., 12 (1991), pp. 399–422.

[9] ———, *A Fornberg-like conformal mapping method for slender regions*, J. Comput. Appl. Math., 46 (1993), pp. 49–64.

[10] T. K. DELILLO, A. R. ELCRAT, AND J. A. PFALTZGRAFF, *Numerical conformal mapping methods based on Faber series*, submitted for publication.

[11] T. K. DELILLO AND J. A. PFALTZGRAFF, *Extremal distance, harmonic measure and numerical conformal mapping*, J. Comput. Appl. Math., 46 (1993), pp. 103–113.

[12] M. DUBINER, *Theoretical and numerical analysis of conformal mapping*, Ph.D thesis, MIT,

Department of Mathematics, Cambridge, MA, 1981.
[13] J. M. FLORYAN AND C. ZEMACH, *Schwarz-Christoffel mappings: a general approach*, J. Comput. Phys., 72 (1987), pp. 347–371.
[14] ———, *Schwarz-Christoffel methods for conformal mapping of regions with a periodic boundary*, J. Comput. Appl. Math., 46 (1993), pp. 77–102.
[15] B. FORNBERG, *A numerical method for conformal mappings*, SIAM J. Sci. Statist. Comput., 1 (1980), pp. 386–400.
[16] D. GAIER, *Konstruktive Methoden der konformen Abbildung*, Springer-Verlag, Berlin, Göttingen, Heidelberg, 1964.
[17] ———, *Ermittlung des konformen Moduls von Vierecken mit Differenzenmethoden*, Numer. Math., 19 (1972), pp. 179–194.
[18] ———, *Ableitungsfreie Abschätzungen bei trigonometrischer Interpolation und Konjugiertenbestimmung*, Computing, 20 (1974), pp. 145–148.
[19] D. GAIER AND W. K. HAYMAN, *Moduli of long quadrilaterals and thick ring domains*, Rend. Mat. Appl. VII, 10 (1990), pp. 809–834.
[20] ———, *On the computation of modules of long quadrilaterals*, Constr. Approx., 7 (1991), pp. 453–467.
[21] E. GRASSMANN, *Numerical experiments with a method of successive approximation for conformal mapping*, Z. Angew. Math. Phys., 30 (1979), pp. 873–884.
[22] M. H. GUTKNECHT, *Numerical experiments on solving Theodorsen's integral equation for conformal maps with the FFT and various nonlinear iterative methods*, SIAM J. Sci. Statist. Comput., 4 (1983), pp. 1–30.
[23] ———, *Numerical conformal mapping methods based on function conjugation*, in Numerical Conformal Mapping, L. N. Trefethen, ed. North-Holland, Amsterdam, 1986, pp. 31–78.
[24] N. D. HALSEY, *Comparison of convergence characteristics of two conformal mapping methods*, AIAA J., 20 (1982), pp. 724–726.
[25] P. HENRICI, *Applied and Computational Complex Analysis, Vol.* III, Wiley, New York, 1986.
[26] C. O. HORGAN, *Book review of "Saint-Venant's Problem" by Dorin Iesan*, SIAM Rev., 31 (1989), pp. 139–141.
[27] D. M. HOUGH, *User's Guide to CONFPACK*, IPS Research Report No. 90-11, ETH, Zurich (1990).
[28] L. H. HOWELL AND L. N. TREFETHEN, *A modified Schwarz-Christoffel transformation for elongated regions*, SIAM J. Sci. Statist. Comput., 11 (1990), pp. 928–949.
[29] O. LEHTO AND K. I. VIRTANEN, *Quasiconformal Mappings in the Plane*, Springer-Verlag, New York, 1973.
[30] D.I. MEIRON, S. A. ORSZAG, AND M. ISRAELI, *Applications of numerical conformal mapping*, J. Comput. Phys., 40 (1981), pp. 345–360.
[31] R. MENIKOFF AND C. ZEMACH, *Methods for numerical conformal mapping*, J. Comput. Phys., 36 (1980), pp. 366–410.
[32] Z. NEHARI, *Conformal Mapping*, McGraw-Hill, New York, 1952.
[33] S. T. O'DONNELL AND V. ROKHLIN, *A fast algorithm for the numerical evaluation of conformal mappings*, SIAM J. Sci. Statist. Comput., 10 (1989), pp. 475–487.
[34] A. M. OSTROWSKI, *Conformal mapping of a special ellipse on the unit circle*, in Experiments in the Computation of Conformal Maps, J. Todd, ed., National Bureau of Standards Applied Mathematics Series, 42 (1955), pp. 1–2.
[35] N. PAPAMICHAEL, *Numerical conformal mapping onto a rectangle with applications to the solution of Laplacian problems*, J. Comput. Appl. Math., 28 (1989), pp. 63–83.
[36] N. PAPAMICHAEL, C. A. KOKKINOS, AND M. K. WARBY, *Numerical techniques for conformal mapping onto a rectangle*, J. Comput. Appl. Math., 20 (1987), pp. 349–358.
[37] N. PAPAMICHAEL AND E. SAFF, EDS., *Special Issue on Computational Complex Analysis*, J. Comput. Appl. Math., 46 (1993).
[38] N. PAPAMICHAEL AND N. S. STYLIANOPOULOS, *On a domain decomposition method for the computation of conformal modules*, Appl. Math. Lett., 1 (1988), pp. 277–280.
[39] ———, *On the numerical performance of a domain decomposition method for conformal mapping*, in Computational Methods and Function Theory, St. Ruscheweyh, E. B. Saff, L. C. Salinas, R. S. Varga, eds., Lecture Notes in Mathematics 1435, Springer-Verlag, Berlin (1990), pp. 155–169.
[40] ———, *A domain decomposition method for conformal mapping onto a rectangle*, Constr. Approx., 7 (1991), pp. 349–379.

[41] N. PAPAMICHAEL AND N. S. STYLIANOPOULOS, *A domain decomposition method for approximating the conformal modules of long quadrilaterals*, Numer. Math., 62 (1992), pp. 213–234.
[42] ———, *On the theory and application of a domain decomposition method for computing conformal modules*, J. Comput. Appl. Math., to appear.
[43] N. PAPAMICHAEL, M. K. WARBY AND D. M. HOUGH, *The treatment of corner and pole-type singularities in numerical conformal mapping techniques*, in Numerical Conformal Mapping, L. N. Trefethen, ed., North-Holland, Amsterdam, 1986, pp. 163–192.
[44] CH. POMMERENKE, *Boundary Behavior of Conformal Maps*, Springer-Verlag, Berlin, Heidelberg, New York, 1992.
[45] R. SCHINZINGER AND P. A. A. LAURA, *Conformal Mapping: Methods and Applications*, Elsevier, Amsterdam, 1991.
[46] L. N. TREFETHEN, ED., *Numerical Conformal Mapping*, North-Holland, Amsterdam; J. Comput. Appl. Math., 14 (1986).
[47] ———, *SCPACK User's Guide*, Numerical Analysis Report 89-2, MIT, Department of Mathematics, Cambridge, MA, 1989.
[48] M. R. TRUMMER, *An efficient implementation of a conformal mapping method based on the Szegö kernel*, SIAM J. Numer. Anal., 23 (1986), pp. 853–872.
[49] E. WEGERT, *An iterative method for solving nonlinear Riemann-Hilbert problems*, J. Comput. Appl. Math., 29 (1990), pp. 311–327.
[50] R. WEGMANN, *Convergence proofs and error estimates for an iterative method for conformal mapping*, Numer. Math., 44 (1984), pp. 435–461.
[51] ———, *Discretized versions of Newton type iterative methods for conformal mapping*, J. Comput. Appl. Math., 29 (1990), pp. 207–224.
[52] ———, *An estimate for crowding in conformal mapping to elongated regions*, Complex Variables, 18 (1992), pp. 193–199.
[53] ———, *Crowding for analytic functions with elongated range*, Constr. Approx., to appear.
[54] E. T. WHITTAKER AND G. N. WATSON, *A Course of Modern Analysis, 4th Edition, reprint*, Cambridge University Press, Cambridge, UK, 1963.
[55] C. ZEMACH, *A conformal map formula for difficult cases*, in Numerical Conformal Mapping, L. N. Trefethen, ed., North-Holland, Amsterdam, 1986, pp. 207–216.
[56] ———, *Limits on the convergence of Fourier expansions of periodic conformal maps*, preprint.